Diminished Ost3-dependent N-glycosylation of the BiP nucleotide exchange factor Sil1 is an adaptive response to reductive ER stress

Kofi L. P. Stevens[a,b], Amy L. Black[a,b], Kelsi M. Wells[a,b], K. Y. Benjamin Yeo[c], Robert F. L. Steuart[b], Colin J. Stirling[d,1], Benjamin L. Schulz[c], and Carl J. Mousley[a,b,2]

[a]School of Biomedical Sciences, Faculty of Health Sciences, Curtin University, Bentley, WA 6102, Australia; [b]Curtin Health Innovation Research Institute and Faculty of Health Sciences, Curtin University, Bentley, WA 6102, Australia; [c]School of Chemistry and Molecular Biosciences, Faculty of Science, University of Queensland, Brisbane St Lucia, QLD 4072, Australia; and [d]Faculty of Life Sciences, University of Manchester, Manchester M13 9PT, United Kingdom

Edited by Armando Parodi, Fundacion Instituto Leloir, Buenos Aries, Argentina, and approved October 3, 2017 (received for review May 10, 2017)

BiP (Kar2 in yeast) is an essential Hsp70 chaperone and master regulator of endoplasmic reticulum (ER) function. BiP's activity is regulated by its intrinsic ATPase activity that can be stimulated by two different nucleotide exchange factors, Sil1 and Lhs1. Both Sil1 and Lhs1 are glycoproteins, but how N-glycosylation regulates their function is not known. Here, we show that N-glycosylation of Sil1, but not of Lhs1, is diminished upon reductive stress. N-glycosylation of Sil1 is predominantly Ost3-dependent and requires a functional Ost3 CxxC thioredoxin motif. N-glycosylation of Lhs1 is largely Ost3-independent and independent of the CxxC motif. Unglycosylated Sil1 is not only functional but is more effective at rescuing loss of Lhs1 activity than N-glycosylated Sil1. Furthermore, substitution of the redox active cysteine pair C52 and C57 in the N terminus of Sil1 results in the Doa10-dependent ERAD of this mutant protein. We propose that reductive stress in the ER inhibits the Ost3-dependent N-glycosylation of Sil1, which regulates specific BiP functions appropriate to the needs of the ER under reductive stress.

N-glycosylation | redox | Sil1 | Ost3 | ERAD

The endoplasmic reticulum (ER) is a major site of protein and lipid biogenesis. Proteins that function within the secretory pathway, or are secreted, are translocated into the ER as unfolded polypeptide chains where they can be N-glycosylated or form disulphide bonds to adopt their mature structures. Fully matured proteins are subsequently transported from the ER to their appropriate destinations. These processes are closely monitored by the ER quality control apparatus to prevent protein aggregation and maintain homeostasis.

The Hsp70 ortholog BiP (Kar2 in yeast) is essential for ER homeostasis, where it acts as a chaperone to promote productive protein folding (1–5). Kar2 activity is regulated by two classes of coregulators; Hsp40/DnaJ-like proteins stimulate ATP hydrolysis, whereas nucleotide exchange factors (NEFs) promote ADP release (6, 7). Together they promote Kar2 activity by allowing it to undergo multiple cycles of substrate binding and release. Cells possess several mechanisms that regulate Kar2 activity to buffer against fluctuations in the ER folding capacity and prevent protein misfolding during ER stress.

ER function relies on the maintenance of an appropriate redox balance. Upon increased ER oxidation, a highly conserved cysteine residue, C63, within the ATPase domain of BiP becomes oxidized (8, 9). This alters BiP/Kar2 chaperone activity to limit polypeptide aggregation during suboptimal redox conditions for ER protein folding (9–11). Reductive stress also gives rise to the accumulation of misfolded proteins. However, little is known regarding the mechanisms that exist to regulate BiP activity during reductive stress, for instance during extensive oxidative protein folding in secretory cells such as pancreatic acinar cells (12).

Here, we show that reductive ER stress diminishes N-glycosylation of the Kar2 NEF Sil1, but not of Lhs1. N-glycosylation of Sil1 is entirely Ost3-dependent and requires a functional CxxC thioredoxin motif. N-glycosylation of Lhs1 is partially Ost3-dependent and independent of the CxxC motif. The unglycosylated Sil1 variant (uSil1) retains functionality and is able to substitute for Lhs1 activity more effectively than its cognate N-glycosylated derivative. We propose that the N-glycosylation status of Sil1 directs the NEF to coordinate specific Kar2-regulated activities to suit the needs of the ER when in a state of reductive stress.

Results

N-Linked Glycosylation of the Sil1 Nucleotide Exchange Factor, but Not of Lhs1, Is Diminished by Reductive Stress. Environmental stress can vary the load of unfolded or misfolded proteins in the ER, so BiP/Kar2 and its effectors must be available and appropriately active in times of need to maintain ER homeostasis. In yeast, treatment with the reductant DTT or the N-glycosylation inhibitor tunicamycin (Tm) increases expression of Kar2 and its NEFs Lhs1 and Sil1 (13). This correlates with an increase in both Sil1 and Lhs1 at the protein level (Fig. 1*A*). Both Lhs1 and Sil1 are N-glycosylated in vegetative cells, and their N-glycosylation is perturbed in cells treated with Tm (Fig. 1*A*). However, we also observed accumulation of unglycosylated Sil1 (uSil1) in cells treated with DTT (Fig. 1*A*). Protease protection analysis ruled out the possibility that cytoplasmic pre-Sil1, rather than uSil1, accumulates in DTT-treated cells (Fig. S1*A*). Also, the predominant form of Sil1 that accumulates upon DTT treatment was not a substrate for the N-glycan–binding lectin Con A (Fig. S1*B*). In

Significance

Endoplasmic reticulum (ER) function relies on the maintenance of an appropriate redox balance. We observe that ER reductive stress is sensed through the oligosaccharyltransferase subunit Ost3 and acts to inhibit glycosylation of Sil1. Misfolded proteins accumulate within the ER under reductive stress and may sequester Lhs1 and limit the pool of free Lhs1 that can function as a BiP nucleotide exchange factor. Furthermore, unglycosylated Sil1 can compensate for the loss of Lhs1 activity more readily than glycosylated Sil1. Accumulation of unglycosylated Sil1 upon reductive stress may therefore be an adaptive mechanism that allows Sil1 to compensate for loss of Lhs1 NEF activity under these conditions.

Author contributions: C.J.S. and C.J.M. designed research; K.L.P.S., A.L.B., K.M.W., and C.J.M. performed research; K.Y.B.Y. and B.L.S. contributed new reagents/analytic tools; K.L.P.S., R.F.L.S., and C.J.M. analyzed data; and K.L.P.S., R.F.L.S., B.L.S., and C.J.M. wrote the paper.

The authors declare no conflict of interest.

This article is a PNAS Direct Submission.

[1]Present address: Office of Vice-Chancellor, Flinders University, Bedford Park, SA 5043, Australia.

[2]To whom correspondence should be addressed. Email: carl.mousley@curtin.edu.au.

This article contains supporting information online at www.pnas.org/lookup/suppl/doi:10.1073/pnas.1705641114/-/DCSupplemental.

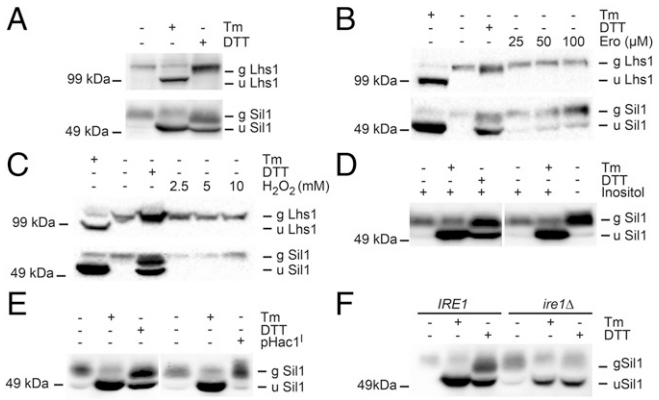

Fig. 1. N-glycosylation of Sil1 is redox sensitive and independent of the UPR. (*A*) Cell extracts derived from WT cells that were either untreated or treated with 10 μg/mL tunicamycin (Tm) or 10 mM DTT for 2 h were immunoblotted with anti-Lhs1 or anti-Sil1 antibodies. (*B*) As *A* but with the inclusion of whole-cell lysates derived from cells treated with the indicated concentrations of erodoxin. (*C*) As *A* but with the inclusion of whole-cell lysates derived from cells treated with the indicated concentrations of H_2O_2. (*D*) Immunoblot analysis of cell extracts derived from WT cells grown in the presence and absence of inositol. For control, cells were untreated or treated with either 10 μg/mL Tm or 10 mM DTT for 2 h. (*E*) Immunoblot analysis of cell lysates derived from WT cells transformed with either pHac1^{I} or vector control. For control, cells were untreated or treated with either 10 μg/mL Tm or 10 mM DTT for 2 h. (*F*) Cell extracts derived from WT and *ire1*Δ cells that were untreated or treated with either 10 μg/mL Tm or 10 mM DTT for 2 h were immunoblotted with anti-Sil1 antibodies.

contrast to Sil1, treatment with DTT did not affect glycosylation of Lhs1 (Fig. 1*A*). This suggested that uSil1 specifically accumulated upon DTT-induced ER stress.

As a reductant, DTT disrupts the redox balance of the ER. The essential Ero1 protein is a thiol oxidase that maintains the ER redox balance required to promote oxidative protein folding in this organelle (14–16). To confirm that Sil1 N-glycosylation is perturbed as a consequence of general ER reductive stress rather than by DTT alone, we investigated Sil1 glycosylation in cells treated with the Ero1 inhibitor 1-bromo-5-methoxy-2,4-dinitrobenzene (Erodoxin) (17). We observe a similar N-glycosylation profile of Sil1 and Lhs1 in cells treated with Erodoxin to that observed in cells treated with DTT, with accumulation of uSil1 but maintenance of efficiently glycosylated Lhs1 (Fig. 1*B*). In contrast to treatments that induce reductive stress, treatment of cells with hydrogen peroxide to impose oxidative stress had no effect on glycosylation of Sil1 or Lhs1 (Fig. 1*C*).

The burden of reductive stress induces the unfolded protein response (UPR). We therefore investigated whether Sil1 N-glycosylation is perturbed in cells in which the UPR is induced by other means. For this, we starved cells of inositol and/or constitutively overexpressed Hac1^{I}. Inositol depletion activates the UPR by disrupting phospholipid homeostasis, while Hac1^{I} is the direct transcriptional activator of the UPR (18, 19). Independent or concurrent inositol depletion or Hac1^{I} overexpression strongly induced the UPR (Fig. S1*C*). Consistent with UPR induction, Sil1 protein levels were substantially increased in inositol-starved cells (Fig. 1*D*) or cells expressing Hac1^{I} (Fig. 1*E*) compared with control cells. However, Sil1 N-glycosylation was not perturbed by either inositol starvation (Fig. 1*D*) or Hac1^{I} expression (Fig. 1*E*). We next tested if inhibition of Sil1 N-glycosylation by reductive stress required a functional UPR. uSil1 accumulated in cells treated with DTT with or without the UPR activator Ire1 (*ire1*Δ) (Fig. 1*F*). Therefore, Sil1 N-glycosylation is not perturbed by general ER stress, but instead is specifically hypersensitive to the redox potential of the ER lumen.

N-Glycosylation of Sil1 Is Ost3-Dependent. Oligosaccharyltransferase (OST) acts at the confluence of protein modification and protein folding. Yeast OST is comprised of eight protein subunits: Ost1, Ost2, Ost4, Ost5, Stt3, Swp1, Wbp1, and either Ost3 or Ost6 (20–23). Ost3 and Ost6 are paralogues, each with distinct substrate specificities, and the incorporation of either into OST defines two isoforms of the enzyme (24). The lumenal domain of both Ost3 and Ost6 possesses a CxxC thioredoxin-like motif, and their redox-dependent peptide binding activities increase the glycosylation efficiency of distinct sites in protein substrates (24). We sought to determine the dependence of Lhs1 and Sil1 N-glycosylation on OST with either Ost3 or Ost6. N-glycosylation of both Lhs1 and Sil1 was not affected in Ost6-deficient cells (*ost6*Δ) (Fig. 2*A*). In contrast, Sil1 was essentially completely unglycosylated in *ost3*Δ cells, indicating that N-glycosylation of Sil1 was predominantly Ost3-dependent (Fig. 2*A*). *ost3Δ* cells also accumulated a form of Lhs1, termed g* Lhs1, with a greater electrophoretic mobility than WT but less than that in cells treated with Tm (Fig. 2*A*). Importantly, no further reduction in glycosylation of Lhs1 was observed in *ost3Δ* cells treated with DTT. This indicated that while N-glycosylation of at least one site in Lhs1 is Ost3-dependent, only Sil1 N-glycosylation is Ost3-dependent and redox sensitive.

The redox sensitivity of Sil1 N-glycosylation suggested the involvement of the Ost3 CxxC thioredoxin-like motif. To test this, we investigated Sil1 N-glycosylation in *ost3*Δ cells expressing Ost3 or a redox inactive variant of Ost3 in which both cysteine residues of the CxxC motif were replaced with serines (*ost3*$^{C\rightarrow S}$). N-glycosylation of Sil1 in *ost3Δ* cells was effectively restored by expression of *OST3* but not with *ost3*$^{C\rightarrow S}$ (Fig. 2*B*). In contrast, N-glycosylation of Lhs1 was restored in cells expressing either *OST3* or *ost3*$^{C\rightarrow S}$ (Fig. 2*B*). This confirms that Sil1 N-glycosylation requires the oxidoreductase activity of the Ost3-containing OST in vivo and that Sil1 N-glycosylation is exquisitely sensitive to the redox status of the ER lumen.

The transient binding of nascent polypeptide to Ost3 and Ost6 proceeds noncovalently or through mixed disulphides and is necessary to inhibit local protein folding to increase N-glycosylation efficiency of substrates (24, 25). The Sil1 protein possesses four cysteine residues (C52, 57, 203, and 373) and six potential N-glycosylation sites (N105, 181, 215, 233, 315, and 333). Sil1 N-glycosylation was not affected by substitution of either C52, C57, C203, or C373 with either alanine or serine (Fig. 2*C*). This was surprising given that Sil1 N-glycosylation is perturbed by reductive stress. Furthermore, the accumulation of uSil1 observed following

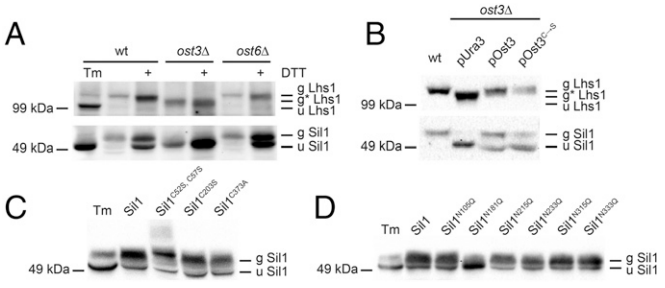

Fig. 2. N-glycosylation of Sil1 is Ost3-dependent. (*A*) Immunoblot analysis of cell extracts derived from either WT, *ost3*Δ, or *ost6*Δ cells that were untreated or treated with either 10 μg/mL Tm or 5 mM DTT for 2 h. (*B*) Immunoblot analysis of cell lysates derived from either WT or *ost3*Δ cells transformed with either vector alone, YCp *OST3*, or YCp *ost3*$^{C\rightarrow S}$. (*C*) Immunoblot analysis of cell lysates derived from *sil1*Δ cells expressing either *SIL1*, *SIL1*$^{C52S,\ C57S}$, *SIL1*^{C203S}, or *SIL1*^{C373S}. For control, cells were treated with 10 μg/mL Tm. (*D*) Immunoblot analysis of cell lysates derived from *sil1*Δ cells expressing either *SIL1*, *SIL1*^{N105Q}, *SIL1*^{N181Q}, *SIL1*^{N215Q}, *SIL*^{N233Q}, *SIL1*^{N315Q}, or *SIL1*^{N333Q}. For control, cells were treated with 10 μg/mL Tm.

DTT treatment was not diminished by substitution of either C52, C57, C203, or C373 with either alanine or serine (Fig. S2*A*). Therefore, the Ost3-dependence of Sil1 N-glycosylation is not bypassed by elimination of a cysteine in Sil1. Glutamine scanning mutagenesis of each potential sequon identified that Sil1 N-glycosylation was only disrupted following substitution of N181 (Fig. 2*D*). Previous studies have shown that disruption of the Ost3 thioredoxin motif only affects the N-glycosylation of a small subset of substrates (24). That no cysteine residue within Sil1 is necessary for N-glycosylation rules out the possibility that reductive stress ablates formation of a mixed disulphide between Ost3 and Sil1. Rather, our data best supports a model in which the substrate-binding domain of Ost3 undergoes a sufficient redox-dependent structural change so that the Sil1 nascent polypeptide is no longer recognized as being a substrate, as has been reported in vitro for model Ost3/Ost6 substrates (24, 25).

Upon further inspection, we realized that Sil1$^{C52S\ C57S}$ had undergone a series of posttranslational modification giving rise to protein laddering (Fig. S2*B*). Such "laddering" is a hallmark of protein polyubiquitination and occurs when ER resident proteins are targeted for ER-associated degradation (ERAD). To investigate whether Sil1$^{C52S\ C57S}$ is turned over, we investigated the stability of Sil1$^{C52S\ C57S}$ and WT Sil1 in cells by cycloheximide (chx) chase analysis. Sil1 protein levels remained constant throughout the 90-min chx chase (Fig. 3 *A* and *B*). In contrast, the Sil1$^{C52S\ C57S}$ protein was more labile as levels diminished throughout the chx chase (Fig. 3 *A* and *B*). We next investigated whether Sil1$^{C52S\ C57S}$ is degraded via ERAD. *DOA10*, and *HRD1*/*DER3* encode for the two major ER resident E3 ligases Doa10 and Hrd1 in yeast (26–28). Deletion of *DOA10* (*doa10Δ*) led to an almost complete stabilization of the Sil1$^{C52S\ C57S}$ protein (Fig. 3 *C* and *D*). Furthermore, expression of *SIL1*$^{C52S\ C57S}$ severely diminished the growth of *doa10Δ* yeast (Fig. 3*E*). In contrast, deletion of *HRD1* (*hrd1Δ*) had no detectable effect on Sil1$^{C52S\ C57S}$ protein stability (Fig. 3 *C* and *D*), and expression of *SIL1*$^{C52S\ C57S}$ did not affect *hrd1Δ* cellular growth (Fig. 3*E*). Deletion of the *HRD3* (*hrd3Δ*) structural gene, which encodes for the Hrd3 component of the HRD complex, also had no detectable effect on Sil1$^{C52S\ C57S}$ protein stability (Fig. 3 *C* and *D*). A role for Doa10 in the degradation of ERAD-L substrates has not been described previously. However, Doa10 has been shown to be required for the degradation of the ERAD-M substrate Sbh2 (29). Given that Sil1$^{C52S\ C57S}$ ERAD is Doa10-dependent, we speculate that Sil1 can associate with the lumenal face of the ER membrane, a hypothesis supported by a previous study showing that the *Yarrowia lipolytica* Sil1 ortholog, Sls1, can be coimmunoprecipitated with Sec61 (30).

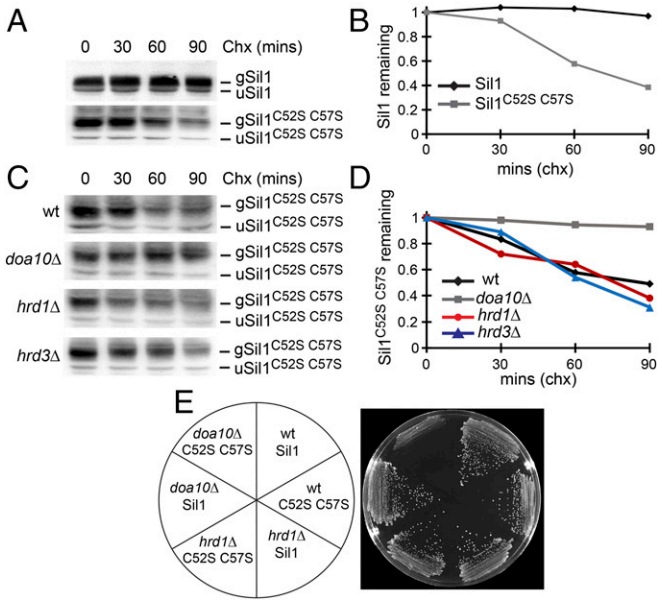

Fig. 3. Sil1$^{C52S,\ C57S}$ is a Doa10 ERAD substrate. (*A*) Exponentially growing *sil1Δ* cells expressing either *SIL1* or *SIL1*$^{C52S,\ C57S}$ were pretreated for 20 min with 0.25 mg/mL chx. Afterward cells were removed at the indicated times and immunoblot analysis of cell lysates performed. (*B*) Densitometric analysis of *A* using Image Lab software (Bio-Rad). (*C*) Exponentially growing WT, *doa10Δ*, *hrd1Δ*, and *hrd3Δ* cells expressing *SIL1*$^{C52S,\ C57S}$ were pretreated for 20 min with 0.25 mg/mL chx. Afterward, cells were removed at the indicated times and immunoblot analysis of cell lysates performed. (*D*) Densitometric analysis of *C* using Image Lab software (Bio-Rad). (*E*) WT, *doa10Δ*, and *hrd1Δ* yeast harboring either YEp *SIL1* or YEp *SIL1*$^{C52S,\ C57S}$ were streaked onto –Leu selective medium and incubated at 30 °C for 2 d.

Unglycosylated Sil1 Is Functional. Individual deletions of *SIL1* (*sil1Δ*) or *LHS1* (*lhs1Δ*) in yeast are viable (31–33), while the double deletion (*sil1Δ lhs1Δ*) is lethal, indicating that Kar2-dependent nucleotide exchange is an essential cellular activity (33). We tested if expression of the unglycosylatable variant *SIL1*^{N181Q} could sustain cell viability in *sil1Δ lhs1Δ* cells. YCp *SIL1* and YCp *SIL1*^{N181Q} were transformed into JTY65 {*sil1Δ::kanMX4 lhs1Δ::kanMX4* [pRC43 (*LHS1*, *URA3*)]} (33) and tested for the ability of these strains to grow after loss of pRC43 on 5-fluoroorotic acid (5-FOA) medium. Strains harboring either *SIL1* or *SIL1*^{N181Q} produced viable colonies, whereas cells transformed with vector alone could not (Fig. 4*A*). This confirmed that unglycosylated Sil1 was functional.

Overexpression of *SIL1* suppresses the severe growth defect of *ire1Δ lhs1Δ* double mutant cells (33). We therefore tested whether overexpression of the *SIL1*^{N181Q} N-glycosylation mutant was able to suppress this growth defect. We transformed YEp *SIL1* and YEp *SIL1*^{N181Q} into JTY62 {*ire1Δ::kanMX4 lhs1Δ::kanMX4* [pJT40 (*LHS1*, *ADE3*, *URA3*)]} and tested the ability of these strains to grow after loss of pJT40 on 5-FOA medium. Again, we observed that overexpression of *SIL1* partially suppresses the severe growth defect of *ire1Δ lhs1Δ* double mutant cells. Surprisingly, overexpression of *SIL1*^{N181Q} allowed a more impressive suppression of this growth defect (Fig. S3*A*). This suggested that under these conditions, uSil1 may compensate for the loss of Lhs1 activity more readily than gSil1. Next, we tested if only modest overexpression of unglycosylatable *SIL1*^{N181Q} was sufficient to rescue the growth defect of *ire1Δ lhs1Δ* cells. This was indeed the case, with low copy expression of *SIL1*^{N181Q} from centrimeric plasmid YCp sufficient to promote growth of JTY62 yeast after induced loss of plasmid-borne *LHS1* expression on 5-FOA medium (Fig. S3*B*). Expression of *SIL1* in the same system only allowed poor growth (Fig. S3*B*). Given the extent to which low copy expression of *SIL1*^{N181Q} was able to promote growth of JTY62 yeast after induced loss of plasmid-borne *LHS1* expression on 5-FOA medium, we tested if expression of *SIL1*^{N181Q} as the only source of *SIL1* was sufficient to rescue the growth defect of *ire1Δ lhs1Δ* cells. A *SIL1*^{N181Q} integration cassette containing the *LEU2* selectable marker was integrated into the *SIL1* genetic locus by homologous recombination, and successful substitution was confirmed by sequencing and immunoblot (Fig. S3 *C* and *D*). Genomic substitution of *SIL1* with *SIL1*^{N181Q}*::LEU2* was sufficient to promote growth of JTY62 yeast after induced loss of plasmid-borne *LHS1* expression on 5-FOA medium (Fig. 4*B*). Together, this shows that unglycosylated Sil1 can compensate for the loss of Lhs1 activity more readily than glycosylated Sil1.

The accumulation of unglycosylated Sil1 upon reductive stress may be necessary to protect cells from this deleterious stress. To test this, we investigated whether low copy expression of *SIL1*^{N181Q} would reduce the hypersensitivity of *ire1Δ* cellular growth to DTT. The rationale for this is that in *ire1Δ* cells, the

CELL BIOLOGY

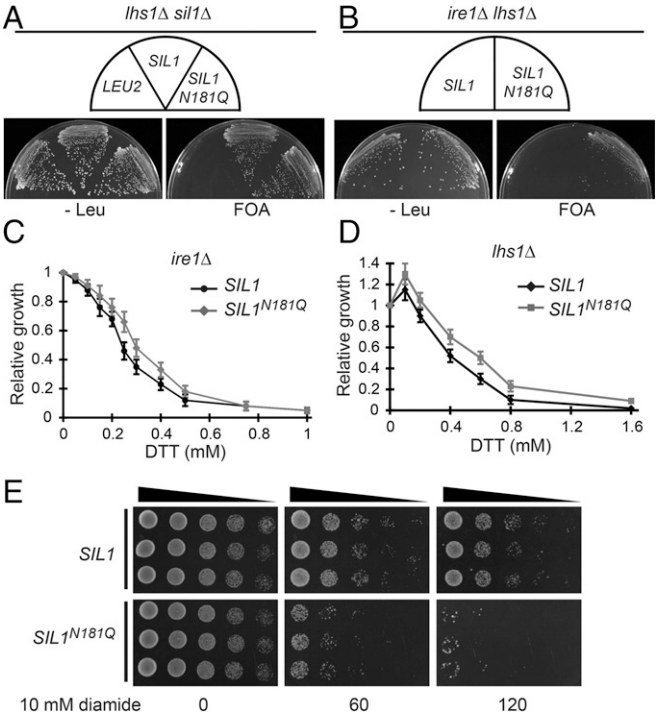

Fig. 4. uSil1 functionally compensates *lhs1Δ* better than gSil1. (*A*) JTY65 yeast harboring either YCp *LEU2*, YCp *SIL1*, or YCp *SIL1*^{N181Q} were streaked onto –Leu selective medium and medium containing FOA and incubated at 30 °C for 2 d. (*B*) JTY62 yeast in which the *SIL1* genetic locus has been substituted with a *SIL1*^{N181Q}*::LEU2* integration cassette and JTY62 parental cells harboring YCp *LEU2* were streaked onto –Leu selective medium and medium containing FOA and incubated at 30 °C for 2 d. (*C*) *ire1Δ* cells harboring either YCp *SIL1* or YCp *SIL1*^{N181Q} were inoculated at 0.01 OD_{600} and grown until control had reached 1 OD_{600}. The relative growth with DTT (0.05–1 mM) relative to "no-DTT" control (ddH_2O) are plotted as function of DTT concentration (*x* axis). Values show mean ± SEM of normalized growth for each DTT concentration from three independent experiments. (*D*) *SIL1 lhs1Δ* and *SIL1*^{N181Q} *lhs1Δ* cells were inoculated at 0.01 OD_{600} and grown until control had reached 1 OD_{600}. The growth with DTT (0.1–1.6 mM) relative to "no-DTT" control (ddH_2O) are plotted as function of DTT concentration (*x* axis). Values show mean ± SEM of normalized growth for each DTT concentration from three independent experiments. (*E*) WT cells harboring either YEp *SIL1* or YEp *SIL1*^{N181Q} were grown to midlog phase. One OD_{600} of cells were incubated with and without 10 mM diamide for 60 and 120 min. Afterward, cells were isolated and washed twice with 5 mL ddH_2O and then recovered in YPD for 8 h. Cells were spotted in a 10-fold dilution series and grown at 30 °C for 2 d.

UPR cannot be induced, and cellular growth is sensitive to concentrations of DTT that negligibly affect Sil1 N-glycosylation. This is important as *SIL1* expression is highly elevated upon UPR induction and would likely mask any beneficial effects of *SIL1*^{N181Q} expression. The relative growth of *ire1Δ* cells transformed with either YCp *SIL1* or YCp *SIL1*^{N181Q} was determined in growth medium containing increasing concentrations of DTT (0.05–1 mM). We observed YCp *SIL1*^{N181Q} to bestow modest suppression of *ire1Δ* DTT hypersensitivity compared with YCp *SIL1* (Fig. 4*C*). We find the growth fitness of *ire1Δ* cells that express *SIL1*^{N181Q} to be ∼1.5× greater than those expressing *SIL1* when exposed to 0.25–0.5 mM DTT (Fig. 4*C*).

lhs1Δ cellular growth is also sensitive to concentrations of DTT that negligibly affect Sil1 N-glycosylation. Given that uSil1 can compensate for the loss of Lhs1 activity more readily than glycosylated Sil1, we were interested to determine whether expression of *SIL1*^{N181Q} would also reduce the hypersensitivity of *lhs1Δ* cellular growth to DTT. We observed *SIL1*^{N181Q} expression to partially suppress *lhs11Δ* DTT hypersensitivity as *lhs1Δ SIL1*^{N181Q} cell growth was greater than *lhs1Δ SIL1* cells at all concentrations of DTT (0.1–1.6 mM) (Fig. 4*D*).

Cells under reductive stress may benefit from uSil accumulation simply because it is more stable than gSil1. We tested this by chx chase analysis in cells that had been acutely challenged with DTT for 1 h. We observed a steady decline in gSil1 protein levels, with ∼70% gSil1 remaining after 90-min chase (Fig. S4 *A* and *B*). However, the decline in uSil1 protein levels over this time course was even more pronounced, with ∼40% uSil1 remaining after 90-min chase (Fig. S4 *A* and *B*). uSil1 is therefore more labile than gSil1 under these conditions. As such, the increased ability of uSil1 to rescue the growth defect of *ire1Δ lhs1Δ* cells and to improve the fitness of *ire1Δ* grown in the presence of DTT is not due to its increased stability.

It has previously been shown that a *sil1Δ* strain exhibits improved survival in the presence of the cysteine oxidant diamide due in part due to the loss of Sil1 NEF activity allowing BiP to reside longer in an ADP/peptide-bound state, thus enhancing BiP's holdase activity (8, 9). Given this, we hypothesized that overexpression of uSil1 would render cells hypersensitive to acute cysteine oxidation evoked by exposure to diamide. To test this, cells overexpressing either *SIL1* or *SIL1*^{N181Q} were either mock treated or exposed to 10 mM diamide for either 1 or 2 h and cell viability was determined following an 8-h recovery in rich media. Indeed, *SIL1*^{N181Q} overexpressing cells were more sensitive to the deleterious effects of diamide, as after 1- or 2-h exposure to 10 mM diamide, ∼100× or 1,000× fewer *SIL1*^{N181Q} overexpressing cells were recovered relative to cells overexpressing *SIL1* (Fig. 4*E*).

Discussion

N-Glycosylation Enables Sil1 Functional Specialization. N-glycosylation and protein folding are intimately linked in the ER. Here, we show that ER reductive stress sensed through Ost3 acts to inhibit glycosylation of Sil1, which increases Sil1's activity as a suppressor of loss of Lhs1. Efficient N-glycosylation under nonstressed conditions is therefore a negative regulator of some aspects of Sil1 function. Genetic or chemical inhibition of N-glycosylation results in widespread underglycosylation of diverse proteins, generally resulting in loss of protein folding efficiency, stability, and function. In contrast, loss of glycosylation of Sil1 results in a gain of function whereby uSil1 is a better Lhs1 substitute than its cognate glycosylated derivative.

It is not obvious how loss of N-glycosylation would alter Sil1 function. The crystal structure of Sil1 shows that N181 is located on the opposite face of Sil1 to the surface that mediates interaction with Kar2 (34). Lack of glycosylation would therefore be unlikely to directly impact interactions between Sil1 and Kar2. However, loss of glycosylation could alter Sil1 structure, flexibility, or dynamics in ways that alter this interaction or that regulate Sil1's NEF activity. It is also possible that loss of glycosylation at N181 specifically impacts interactions between Sil1 and other proteins.

Although Sil1 and Lhs1 are functionally related, they are not entirely interchangeable, as some mutant phenotypes remain upon cross-complementation even with high levels of overexpression. Genetic interaction networks are distinct for *lhs1Δ* and *sil1Δ* cells (17, 35–45), further suggesting Lhs1 and Sil1 have some specialized function(s). We consider the N-glycosylation of Sil1 to be an important factor that enables regulation of such functional specialization. For example, Lhs1 can also act as an ATP-independent holdase, binding to misfolded proteins to prevent them from aggregating (46–48). The accumulation of misfolded proteins in the ER under reductive stress may sequester Lhs1 and limit the pool of free Lhs1 that can function as a NEF. Given that uSil1 is a better substitute for Lhs1, accumulation of unglycosylated Sil1 upon reductive stress may allow Sil1 to either compensate for loss of Lhs1 NEF activity or to

bolster NEF activity in ER functions coordinated by Lhs1 under these conditions.

Sil1, a Redox-Dependent ERAD Substrate? It is the accepted model that ERAD-L substrates are exclusively recognized by the Hrd1 complex, and ERAD-C substrates by the Doa10 complex (29, 49–53). As Sil1 does not possess a transmembrane domain, we predicted Sil1$^{C52S\ C57S}$ would be a Hrd1-dependent ERAD-L substrate. However, the supposition that ERAD-L and ERAD-C substrates are exclusively recognized by the Hrd1 complex and Doa10 complex, respectively, is derived from analysis of a limited number of ERAD substrates. Our observation that ERAD of Sil1$^{C52S\ C57S}$ is Doa10-dependent suggests that this model is incomplete, and there may well be more unidentified Doa10-dependent ER lumenal substrates. Another possibility is that membrane association of lumenal proteins can drive Doa10-dependent ERAD. It has recently been shown that Doa10 is required for degradation of the ERAD-M substrate Sbh2 (29). Sbh2 is the first characterized Doa10 substrate for which its TM domain and short ER-lumenal domain can target the protein for Doa10-dependent degradation (29). It is possible that Sil1 associates predominantly with the lumenal face of the ER membrane, and it is this association that enables Sil1$^{C52S\ C57S}$ to be a Doa10 ERAD substrate. We attempted to test if N-glycosylation is necessary for Doa10-dependent ERAD of Sil1$^{C52S\ C57S}$, but the pool of uSil1$^{C52S\ C57S}$ that accumulates upon tunicamycin treatment undergoes rapid additional posttranslational modification, making analysis impossible (Fig. S2*C*). However, uSil1 turnover is faster than gSil1 in DTT-treated cells, showing that N-glycosylation is not required for Sil1 turnover.

Residues C52 and C57 of Sil1 have recently been shown to form a redox-active cysteine pair that facilitates the reduction of C63 in the ATPase domain of Kar2 (8). Oxidation of C63 impairs Kar2's ATPase activity, altering its chaperone function to cope with the suboptimal folding conditions that arise during oxidative stress (8–11). Sil1 can then reduce the oxidized cysteine residue in the BiP ATPase domain to restore ATPase activity and chaperone function once the levels of oxidative stress in the ER have subsided. Inappropriate reduction of Kar2 C63 by Sil1 under oxidative stress would therefore be undesirable. Our observation that Sil1$^{C52S,\ C57S}$ is an ERAD substrate suggests that Sil1 degradation is redox-dependent, with the Sil1$^{C52S,\ C57S}$ variant simulating the Sil1 N terminus in its fully reduced state. In addition, we frequently observe Sil1 turnover to be more pronounced in DTT-treated cells relative to control. The redox-dependent degradation of Sil1 may therefore appropriately limit the amount of Sil1 that has the potential to reduce C63 in the ATPase domain of Kar2/BiP, such as when Kar2 is required to function as a holdase.

Concluding Remarks

With their ER-lumenal thioredoxin-like domains, the Ost3 and Ost6 subunits of OST integrate protein modification and protein folding of diverse substrates across the cellular glycoproteome. Our discovery that the redox status of Ost3 controls the N-glycosylation of the ER lumenal Sil1 nucleotide exchange factor also places this OST subunit at the heart of ER protein folding homeostasis. Based on our data, we propose a model in which ER reductive stress reduces the Ost3 CxxC motif, inhibiting N-glycosylation of Sil1 to modulate its activity such that Kar2 function can be tailored to suit the needs of the ER. Furthermore, the apparent hypersensitivity of Sil1 N-glycosylation to reductive stress may provide a simple assay to monitor the redox environment of the ER.

Materials and Methods

Strain and Growth Conditions. *Saccharomyces cerevisiae* strains are listed in Table S1, and plasmids are listed in Table S2. Yeast strains were grown routinely at 30 °C in YP medium (2% peptone, 1% yeast extract) containing 2% glucose (YPD) or in minimal medium (0.67% yeast nitrogen base; YNB) with 2% glucose plus appropriate supplements for selective growth. All media were from Difco Laboratories. Yeast transformations and 5-FOA counter-selection of *URA3* cells were carried out as described previously (54). Cell density in liquid culture was monitored by A_{600} using an Eppendorf Biophotometer.

Immunoblotting. Whole yeast extracts were prepared by glass bead lysis in SDS sample buffer from cultures grown to mid-log phase, resolved by SDS/PAGE, transferred to a nitrocellulose membrane (Bio-Rad), and probed with either αLhs1, αKar2, or αSil1 antiserum whose production has been described previously (33). These antibodies were used at the dilutions indicated in parentheses for immunoblotting: Lhs1 (sheep, 1:10000), Kar2 (sheep, 1:10000), Sil1 (sheep, 1:5000) peroxidase-conjugated goat anti-sheep IgG (1:10000; Sigma). Immunoreactive species were visualized using Clarity (Bio-Rad), and protein degradation rates were determined using a ChemiDoc imaging system (Bio-Rad) and Image Lab software (Bio-Rad).

Chx Chase Analyses. Chx chase analyses were performed according to Habeck et al. (29). Briefly, 0.25 mg/mL chx was added to log-phase yeast cultures, and cell aliquots were removed at the indicated times after addition. Cells were harvested by centrifugation and resuspended in ice cold 10 mM NaN_3. After preparation of lysates, proteins were separated by SDS/PAGE and immunodetection was performed as described above.

ACKNOWLEDGMENTS. This work was supported by a Curtin University Faculty of Health Sciences start-up fund (to C.J.M.).

1. Brodsky JL, et al. (1999) The requirement for molecular chaperones during endoplasmic reticulum-associated protein degradation demonstrates that protein export and import are mechanistically distinct. *J Biol Chem* 274:3453–3460.
2. Corsi AK, Schekman R (1997) The lumenal domain of Sec63p stimulates the ATPase activity of BiP and mediates BiP recruitment to the translocon in Saccharomyces cerevisiae. *J Cell Biol* 137:1483–1493.
3. Matlack KE, Misselwitz B, Plath K, Rapoport TA (1999) BiP acts as a molecular ratchet during posttranslational transport of prepro-alpha factor across the ER membrane. *Cell* 97:553–564.
4. Nishikawa SI, Fewell SW, Kato Y, Brodsky JL, Endo T (2001) Molecular chaperones in the yeast endoplasmic reticulum maintain the solubility of proteins for retrotranslocation and degradation. *J Cell Biol* 153:1061–1070.
5. Simons JF, Ferro-Novick S, Rose MD, Helenius A (1995) BiP/Kar2p serves as a molecular chaperone during carboxypeptidase Y folding in yeast. *J Cell Biol* 130:41–49.
6. Liberek K, Marszalek J, Ang D, Georgopoulos C, Zylicz M (1991) Escherichia coli DnaJ and GrpE heat shock proteins jointly stimulate ATPase activity of DnaK. *Proc Natl Acad Sci USA* 88:2874–2878.
7. Szabo A, et al. (1994) The ATP hydrolysis-dependent reaction cycle of the Escherichia coli Hsp70 system DnaK, DnaJ, and GrpE. *Proc Natl Acad Sci USA* 91:10345–10349.
8. Siegenthaler KD, Pareja KA, Wang J, Sevier CS (2017) An unexpected role for the yeast nucleotide exchange factor Sil1 as a reductant acting on the molecular chaperone BiP. *Elife* 6:e24141.
9. Wang J, Pareja KA, Kaiser CA, Sevier CS (2014) Redox signaling via the molecular chaperone BiP protects cells against endoplasmic reticulum-derived oxidative stress. *Elife* 3:e03496.
10. Wang J, Sevier CS (2016) Formation and reversibility of BiP protein cysteine oxidation facilitate cell survival during and post oxidative stress. *J Biol Chem* 291:7541–7557.
11. Xu M, Marsh HM, Sevier CS (2016) A conserved cysteine within the ATPase domain of the endoplasmic reticulum chaperone BiP is necessary for a complete complement of BiP activities. *J Mol Biol* 428:4168–4184.
12. Maity S, et al. (2016) Oxidative homeostasis regulates the response to reductive endoplasmic reticulum stress through translation control. *Cell Rep* 16:851–865.
13. Travers KJ, et al. (2000) Functional and genomic analyses reveal an essential coordination between the unfolded protein response and ER-associated degradation. *Cell* 101:249–258.
14. Frand AR, Kaiser CA (1998) The ERO1 gene of yeast is required for oxidation of protein dithiols in the endoplasmic reticulum. *Mol Cell* 1:161–170.
15. Pollard MG, Travers KJ, Weissman JS (1998) Ero1p: A novel and ubiquitous protein with an essential role in oxidative protein folding in the endoplasmic reticulum. *Mol Cell* 1:171–182.
16. Sevier CS, et al. (2007) Modulation of cellular disulfide-bond formation and the ER redox environment by feedback regulation of Ero1. *Cell* 129:333–344.
17. Costanzo M, et al. (2010) The genetic landscape of a cell. *Science* 327:425–431.
18. Gaspar ML, Aregullin MA, Jesch SA, Henry SA (2006) Inositol induces a profound alteration in the pattern and rate of synthesis and turnover of membrane lipids in Saccharomyces cerevisiae. *J Biol Chem* 281:22773–22785.
19. Kelley MJ, Bailis AM, Henry SA, Carman GM (1988) Regulation of phospholipid biosynthesis in Saccharomyces cerevisiae by inositol. Inositol is an inhibitor of phosphatidylserine synthase activity. *J Biol Chem* 263:18078–18085.

20. Karaoglu D, Kelleher DJ, Gilmore R (1995) Functional characterization of Ost3p. Loss of the 34-kD subunit of the Saccharomyces cerevisiae oligosaccharyltransferase results in biased underglycosylation of acceptor substrates. *J Cell Biol* 130:567–577.
21. Kelleher DJ, Gilmore R (2006) An evolving view of the eukaryotic oligosaccharyltransferase. *Glycobiology* 16:47R–62R.
22. Schwarz M, Knauer R, Lehle L (2005) Yeast oligosaccharyltransferase consists of two functionally distinct sub-complexes, specified by either the Ost3p or Ost6p subunit. *FEBS Lett* 579:6564–6568.
23. Spirig U, Bodmer D, Wacker M, Burda P, Aebi M (2005) The 3.4-kDa Ost4 protein is required for the assembly of two distinct oligosaccharyltransferase complexes in yeast. *Glycobiology* 15:1396–1406.
24. Schulz BL, et al. (2009) Oxidoreductase activity of oligosaccharyltransferase subunits Ost3p and Ost6p defines site-specific glycosylation efficiency. *Proc Natl Acad Sci USA* 106:11061–11066.
25. Jamaluddin MF, Bailey UM, Schulz BL (2014) Oligosaccharyltransferase subunits bind polypeptide substrate to locally enhance N-glycosylation. *Mol Cell Proteomics* 13: 3286–3293.
26. Bordallo J, Plemper RK, Finger A, Wolf DH (1998) Der3p/Hrd1p is required for endoplasmic reticulum-associated degradation of misfolded lumenal and integral membrane proteins. *Mol Biol Cell* 9:209–222.
27. Hampton RY, Gardner RG, Rine J (1996) Role of 26S proteasome and HRD genes in the degradation of 3-hydroxy-3-methylglutaryl-CoA reductase, an integral endoplasmic reticulum membrane protein. *Mol Biol Cell* 7:2029–2044.
28. Swanson R, Locher M, Hochstrasser M (2001) A conserved ubiquitin ligase of the nuclear envelope/endoplasmic reticulum that functions in both ER-associated and Matalpha2 repressor degradation. *Genes Dev* 15:2660–2674.
29. Habeck G, Ebner FA, Shimada-Kreft H, Kreft SG (2015) The yeast ERAD-C ubiquitin ligase Doa10 recognizes an intramembrane degron. *J Cell Biol* 209:261–273.
30. Boisramé A, Beckerich JM, Gaillardin C (1996) Sls1p, an endoplasmic reticulum component, is involved in the protein translocation process in the yeast Yarrowia lipolytica. *J Biol Chem* 271:11668–11675.
31. Craven RA, Egerton M, Stirling CJ (1996) A novel Hsp70 of the yeast ER lumen is required for the efficient translocation of a number of protein precursors. *EMBO J* 15: 2640–2650.
32. Steel GJ, Fullerton DM, Tyson JR, Stirling CJ (2004) Coordinated activation of Hsp70 chaperones. *Science* 303:98–101.
33. Tyson JR, Stirling CJ (2000) LHS1 and SIL1 provide a lumenal function that is essential for protein translocation into the endoplasmic reticulum. *EMBO J* 19:6440–6452.
34. Yan M, Li J, Sha B (2011) Structural analysis of the Sil1-Bip complex reveals the mechanism for Sil1 to function as a nucleotide-exchange factor. *Biochem J* 438: 447–455.
35. Sharifpoor S, et al. (2012) Functional wiring of the yeast kinome revealed by global analysis of genetic network motifs. *Genome Res* 22:791–801.
36. Jonikas MC, et al. (2009) Comprehensive characterization of genes required for protein folding in the endoplasmic reticulum. *Science* 323:1693–1697.
37. Schuldiner M, et al. (2005) Exploration of the function and organization of the yeast early secretory pathway through an epistatic miniarray profile. *Cell* 123:507–519.
38. Bircham PW, et al. (2011) Secretory pathway genes assessed by high-throughput microscopy and synthetic genetic array analysis. *Mol Biosyst* 7:2589–2598.
39. Hoppins S, et al. (2011) A mitochondrial-focused genetic interaction map reveals a scaffold-like complex required for inner membrane organization in mitochondria. *J Cell Biol* 195:323–340.
40. Krogan NJ, et al. (2006) Global landscape of protein complexes in the yeast Saccharomyces cerevisiae. *Nature* 440:637–643.
41. Wang Y, et al. (2012) Coiled-coil networking shapes cell molecular machinery. *Mol Biol Cell* 23:3911–3922.
42. Ho Y, et al. (2002) Systematic identification of protein complexes in Saccharomyces cerevisiae by mass spectrometry. *Nature* 415:180–183.
43. McClellan AJ, et al. (2007) Diverse cellular functions of the Hsp90 molecular chaperone uncovered using systems approaches. *Cell* 131:121–135.
44. Batisse J, Batisse C, Budd A, Böttcher B, Hurt E (2009) Purification of nuclear poly(A)-binding protein Nab2 reveals association with the yeast transcriptome and a messenger ribonucleoprotein core structure. *J Biol Chem* 284:34911–34917.
45. Tarassov K, et al. (2008) An in vivo map of the yeast protein interactome. *Science* 320: 1465–1470.
46. Behnke J, Hendershot LM (2014) The large Hsp70 Grp170 binds to unfolded protein substrates in vivo with a regulation distinct from conventional Hsp70s. *J Biol Chem* 289:2899–2907.
47. Buck TM, et al. (2013) The Lhs1/GRP170 chaperones facilitate the endoplasmic reticulum-associated degradation of the epithelial sodium channel. *J Biol Chem* 288: 18366–18380.
48. de Keyzer J, Steel GJ, Hale SJ, Humphries D, Stirling CJ (2009) Nucleotide binding by Lhs1p is essential for its nucleotide exchange activity and for function in vivo. *J Biol Chem* 284:31564–31571.
49. Zattas D, Hochstrasser M (2015) Ubiquitin-dependent protein degradation at the yeast endoplasmic reticulum and nuclear envelope. *Crit Rev Biochem Mol Biol* 50: 1–17.
50. Ruggiano A, Foresti O, Carvalho P (2014) Quality control: ER-associated degradation: Protein quality control and beyond. *J Cell Biol* 204:869–879.
51. Rubenstein EM, Kreft SG, Greenblatt W, Swanson R, Hochstrasser M (2012) Aberrant substrate engagement of the ER translocon triggers degradation by the Hrd1 ubiquitin ligase. *J Cell Biol* 197:761–773.
52. Brodsky JL, Skach WR (2011) Protein folding and quality control in the endoplasmic reticulum: Recent lessons from yeast and mammalian cell systems. *Curr Opin Cell Biol* 23:464–475.
53. Hirsch C, Gauss R, Horn SC, Neuber O, Sommer T (2009) The ubiquitylation machinery of the endoplasmic reticulum. *Nature* 458:453–460.
54. Wilkinson BM, Tyson JR, Reid PJ, Stirling CJ (2000) Distinct domains within yeast Sec61p involved in post-translational translocation and protein dislocation. *J Biol Chem* 275:521–529.
55. Rothblatt JA, Meyer DI (1986) Secretion in yeast: Reconstitution of the translocation and glycosylation of alpha-factor and invertase in a homologous cell-free system. *Cell* 44:619–628.
56. Winzeler EA, et al. (1999) Functional characterization of the S. cerevisiae genome by gene deletion and parallel analysis. *Science* 285:901–906.
57. Chapman RE, Walter P (1997) Translational attenuation mediated by an mRNA intron. *Curr Biol* 7:850–859.